

基于拉氏反变换的传输线耦合电流半解析解

卢斌先, 王泽忠, 程养春

(高电压与电磁兼容北京市重点实验室(华北电力大学), 北京市 昌平区 102206)

Laplace Inverse Transformation Based Semi-Analytical Solution of Coupling Currents of Transmission Line Illuminated by Electromagnetic Pulse

LU Bin-xian, WANG Ze-zhong, CHENG Yang-chun

(Beijing Key Laboratory of High Voltage & EMC (North China Electric Power University), Haidian District, Beijing 102206, China)

ABSTRACT: According to the characteristics of the uniform plane wave, the distributed source generated on transmission line by external field can be regarded as the source delayed by that at the sending terminal. This retardation is the function of incident parameters of external field. On the basis of Taylor transmission line model and considering the retardation of distributed exciting sources under the excitation of uniform plane wave, the formulae of semi-analytical solution of current at receiving terminal of transmission line, which is composed of single lossless conductor and ideal ground, are derived in the Laplace domain; then by use of the property of Laplace inverse transformation, the semi-analytical solution of current in time domain is derived. Terminal coupling current varies with the transmission line parameters and incident parameter of spatial electromagnetic field. Simulation results show that the derived formulae for semi-analytical solution can converge quickly, and the derived formulae are available for reference to the research on the coupling mechanism of electromagnetic field to transmission line and on effect of parameters on the magnitude of coupling current.

KEY WORDS: coupling ; semi analytical solution ; transmission line ; electromagnetic pulse ; Laplace transformation

摘要: 根据均匀平面波的特点, 可将外场激励下传输线沿线激励的电源视为传输线首端等效电源的延迟, 该延迟是空间电磁场相对于传输线入射参数的函数。基于 Taylor 传输线耦合模型, 考虑均匀平面波激励下分布激励源的延迟性, 推导了以理想大地为回线拉普拉斯域的传输线终端电流的半解析解公式, 然后应用拉普拉斯反变换的性质推导出了时域电流的半解析解。终端耦合电流随着传输线参数和空间电磁

场入射参数的变化而变化。仿真结果表明该半解析解公式收敛很快, 对分析研究电磁场在传输线上的耦合机理和研究影响耦合电流大小的参数有特别意义。

关键词: 耦合; 半解析解; 传输线; 电磁脉冲; 拉普拉斯变换

0 引言

随着电力系统自动化程度的不断提高和保护与控制设备的下放, 变电站中保护与控制设备抗电磁干扰问题越来越受到重视。开关操作、电力系统不对称故障和雷击产生的瞬态强电磁脉冲场是变电站中主要的空间电磁干扰源^[1-3]。线缆作为变电站现场与保护小室的重要联络设备, 绝大部分暴露于空气中, 因此空间电磁场与传输线之间的耦合问题是电磁兼容的重要问题之一。由于传输线模型简单, 且易于考虑参数的频变特性, 因此在电磁场与线缆耦合问题中得到了广泛的应用。传输线模型主要包括 Taylor 模型^[4]、Agrawal 模型^[5]和 Racchidi 模型^[6]。由于场线耦合问题复杂, 相关参数较多, 因此不便于研究耦合机理^[7-15]; 而在实际应用中, 常会遇到单导体与参考导体组成的传输线, 导体电导率很高, 可视为理想导体。本文基于传输线 Taylor 模型推导了均匀平面波在传输线终端的耦合电流公式, 并进行了验证, 分析了该方法的收敛速度。由于该公式为半解析解, 该方法对分析研究电磁场在传输线上的耦合机理和各参数对耦合电流大小的影响有着特别意义。

1 场线耦合的拉斯域传输线模型

传输线如图 1 所示。入射角(相对于 y 轴正方向)为 θ , 方位角(相对于 x 轴负方向)为 f , 极化角为 a ,

基金项目: 国家杰出青年科学基金资助项目(50325723)。

Scientific Funds for Outstanding Young Scientists of China
(50325723).

时域 Taylor 传输线耦合模型为^[16]

$$\begin{bmatrix} \frac{\partial u(x,t)}{\partial x} \\ \frac{\partial i(x,t)}{\partial x} \end{bmatrix} + \begin{bmatrix} 0 & L \\ C & 0 \end{bmatrix} \begin{bmatrix} \frac{\partial u(x,t)}{\partial t} \\ \frac{\partial i(x,t)}{\partial t} \end{bmatrix} = - \begin{bmatrix} u_f(x,t) \\ i_f(x,t) \end{bmatrix} \quad (1)$$

式中: $u(x, t)$ 和 $i(x, t)$ 分别为传输线沿线电压和电流; L 和 C 分别为传输线单位长度电感和电容; $u_f(x, t)$ 和 $i_f(x, t)$ 分别为空间电磁场在传输线沿线上等效分布电压源和电流源, 表达式为

$$u_f(x, t) = \frac{\partial}{\partial t} \int_0^h B_z(x, y, t) dy \quad (2)$$

$$i_f(x, t) = C \frac{\partial}{\partial t} \int_0^h E_y(x, y, t) dy \quad (3)$$

式中: E 和 B 分别为电场和磁场; 下标表示相应分量; 上标 e 表示外加电磁场; h 为导体距地面的高度。式(1)的拉氏域解为^[16]

$$\begin{bmatrix} U(x_2, s) \\ I(x_2, s) \end{bmatrix} = F(x_2 - x_1) \begin{bmatrix} U(x_1, s) \\ I(x_1, s) \end{bmatrix} - \int_{x_1}^{x_2} F(x_2 - x) \begin{bmatrix} U_f(x, s) \\ I_f(x, s) \end{bmatrix} dx \quad (4)$$

式中 $F(x)$ 为转换矩阵

$$F(x) = \begin{bmatrix} \cosh(sx/c) & -Z_0 \sinh(sx/c) \\ -1/Z_0 \sinh(sx/c) & \cosh(sx/c) \end{bmatrix} \quad (5)$$

式中: x_1 和 x_2 为传输线沿 x 方向的首末端坐标; s 为拉普拉斯算子; $Z_0 = \sqrt{L/C}$ 为传输线的特性阻抗; c 为电磁波传播的速度。推导得电流时域解

$$\begin{aligned} & \int_{x_1}^{x_2} \exp[-s(r + x \cos f \sin q)/c] [\cosh s(x_2 - x)/c] dx = \\ & \frac{\cos f \sin q \exp[-s(r + x_2 \cos f \sin q)/c]}{s(1 - \cos^2 f \sin^2 q)/c} + \\ & \frac{(1 - \cos f \sin q)}{2} \cdot \exp[-s(r + x_1 \cos f \sin q - l)/c] - \\ & \frac{(1 + \cos f \sin q)}{2} \exp[-s(r + x_1 \cos f \sin q + l)/c] \end{aligned} \quad (6)$$

$$\begin{aligned} & \int_{x_1}^{x_2} \exp[-s(r + x \cos f \sin q)/c] [\sinh s(x_2 - x)/c] dx = \\ & \frac{1}{s(1 - \cos^2 f \sin^2 q)/c} \{-\exp[-s(r + x_2 \cos f \sin q)/c] + \\ & \frac{(1 - \cos f \sin q)}{2} \exp[-s(r + x_1 \cos f \sin q - l)/c] + \\ & \frac{(1 + \cos f \sin q)}{2} \exp[-s(r + x_1 \cos f \sin q + l)/c]\} \end{aligned} \quad (7)$$

式中: f 和 q 分别为入射电磁场的方位角和仰角(如图 1 所示); l 为传输线长度; r 为计时起点入射电磁波的波头到坐标原点的距离。

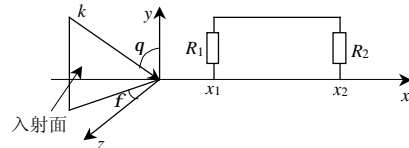


图 1 空间电磁场与传输线的相对位置
Fig. 1 Diagram of relative position between electromagnetic field and transmission line

基于式(5)~(7)可推导出首端电流

$$\begin{aligned} I_1(s) = & \frac{2Z_0c}{\sqrt{(R_1^2 - Z_0^2)(R_2^2 - Z_0^2)} \cdot (1 - \cos^2 f \sin^2 q)} \cdot \\ & \sum_{n=0}^{\infty} (I)^n \exp[-(2n+1)(sl/c + a \tanh M)] \cdot \{\exp \\ & [-s(r + x_2 \cos f \sin q)/c][A_1 + (A_2 + A_3)hE_y(s)] + \\ & \frac{(1 - \cos f \sin q)}{2} \exp[-s(r + x_1 \cos f \sin q - l)/c] \cdot \\ & [B_1 + (B_2 + B_3)hE_y(s)] - \frac{(1 + \cos f \sin q)}{2} \\ & \exp[-s(r + x_1 \cos f \sin q + l)/c] \cdot \\ & [C_1 + (C_2 + C_3)hE_y(s)]\} \end{aligned} \quad (8)$$

式中: $A = R_1 + R_2$, $B = Z_0 + R_1 R_2 / Z_0$, R_1 和 R_2 分别为传输线首端和末端端接电阻; $A > B$ 时 $I = -1$, $M = B/A$; $B > A$ 时 $I = 1$, $M = A/B$; $A_1 = (\cos f \sin q - R_2/Z_0)E_x(s)/s$; $A_2 = (\cos f \sin q/c + R_2 C) \cdot \cos f \sin q$; $A_3 = -(Z_0 C + R_2 \cos f \sin q/(Z_0 c))$; $B_1 = E_x(s)(1 + R_2/Z_0)/s$; $B_2 = \cos f \sin q/c(1 + R_2/Z_0)$; $B_3 = Z_0 C(1 + R_2/Z_0)$; $C_1 = E_x(s)(1 - R_2/Z_0)/s$; $C_2 = \cos f \sin q/c(1 - R_2/Z_0)$; $C_3 = -Z_0 C(1 - R_2/Z_0)$ 。

$$\text{令 } k_0 = \frac{2c}{1 - \cos^2 f \sin^2 q} \frac{Z_0}{\sqrt{(R_1^2 - Z_0^2)(R_2^2 - Z_0^2)}};$$

$T_0 = l/c$, $T_1 = (r + x_1 \cos f \sin q)/c$; $T_2 = (r + x_2 \cos f \sin q)/c$ 。末端电流为

$$\begin{aligned} I_2(s) = & \frac{2Z_0c}{\sqrt{(R_1^2 - Z_0^2)(R_2^2 - Z_0^2)}(1 - \cos^2 f \sin^2 q)} \cdot \\ & \sum_{n=0}^{\infty} (I)^n \exp[-(2n+1)(sl/c + a \tanh M)] \cdot \{\exp[-s \\ & (r + x_2 \cos f \sin q)/c][D_1 + (D_2 + D_3) \cdot hE_y(s)] - \\ & \frac{(1 - \cos f \sin q)}{2} \exp[-s(T_2 + (2n+2)T_0)] \cdot \\ & [E_1 + (E_2 + E_3)hE_y(s)] + \frac{(1 + \cos f \sin q)}{2} \\ & \exp[-s(T_2 + 2nT_0)][F_1 + (F_2 + F_3)hE_y(s)]\} \end{aligned} \quad (9)$$

式中: $D_1 = -(\cos f \sin q + R_1/Z_0)E_x(s)/s$; $D_2 = (1 - R_1/Z_0)\cos f \sin q/c$; $D_3 = (1 - R_1/Z_0)CZ_0$; $E_1 =$

$$\begin{aligned} E_x(s)(1-R_1/Z_0)/s &; \quad E_2 = (1-R_1/Z_0)\cos f \sin q / c; \\ E_3 = (1-R_1/Z_0)CZ_0 &; \quad F_1 = E_x(s)(1+R_1/Z_0)/s; \quad F_2 = \cos f \sin q / c(1+R_1/Z_0); \\ F_3 = -CZ_0(1+R_1/Z_0) + R_1 \cos f \sin q / (cZ_0). \end{aligned}$$

2 理想大地为回线时耦合电流时域解

2.1 理论公式

对于大多数由良导体组成的传输线来说, 可将该传输线视为无损耗传输线。 $e(t)$ 为电场强度的时域表达式, 式(8)(9)经过拉普拉斯反变换, 并写成向量的形式为

$$i_1(t) = k_0 \sum_{n=0}^{\infty} (I)^n e^{-(2n+1)\arctanh M} (\mathbf{K}_{x1}^T \mathbf{S}_{x1} + \mathbf{K}_{y1}^T \mathbf{S}_{y1}) \quad (10)$$

$$\text{式中: } \mathbf{K}_{x1} = [k_1(1+\frac{R_2}{Z_0}), \cos f \sin q - \frac{R_2}{Z_0}, -k_2(1-\frac{R_2}{Z_0})]^T;$$

$$\mathbf{S}_{x1} = \left[\int_0^t e_x[t - (T_1 + 2nT_0)] dt \right. \\ \left. \int_0^t e_x[t - (T_2 + (2n+1)T_0)] dt \right]; \\ \left. \int_0^t e_x[t - (T_1 + (2n+2)T_0)] dt \right]$$

$$\mathbf{K}_{y1} = \left[k_1(1+\frac{R_2}{Z_0})(\cos f \sin q / c + Z_0 C) \right. \\ \left. \cos f \sin q / c(\cos f \sin q - \frac{R_2}{Z_0}) - \right. \\ \left. Z_0 C(1-\frac{R_2}{Z_0} \cos f \sin q) \right. \\ \left. -k_2(1-\frac{R_2}{Z_0})(\cos f \sin q / c - Z_0 C) \right]$$

$$\mathbf{S}_{y1} = \left[h e_y[t - (T_1 + 2nT_0)] \right. \\ \left. h e_y[t - (T_2 + (2n+1)T_0)] \right]; \\ \left. h e_y[t - (T_1 + (2n+2)T_0)] \right]$$

$$k_1 = (1 - \cos f \sin q) / 2; \quad k_2 = (1 + \cos f \sin q) / 2.$$

$$i_2(t) = k_0 \sum_{n=0}^{\infty} (I)^n e^{-(2n+1)\arctanh M} (\mathbf{K}_{x2}^T \mathbf{S}_{x2} + \mathbf{K}_{y2}^T \mathbf{S}_{y2}) \quad (11)$$

式中:

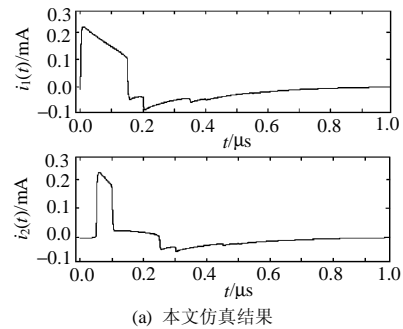
$$\mathbf{K}_{x2} = \left[k_2 \left(1 + \frac{R_1}{Z_0} \right), -\cos f \sin q - \frac{R_1}{Z_0}, -k_1 \left(1 - \frac{R_2}{Z_0} \right) \right]^T;$$

$$\mathbf{S}_{x2} = \left[\int_0^t e_x[t - (T_2 + 2nT_0)] dt \right. \\ \left. \int_0^t e_x[t - (T_1 + (2n+1)T_0)] dt \right]; \\ \left. \int_0^t e_x[t - (T_2 + (2n+2)T_0)] dt \right]$$

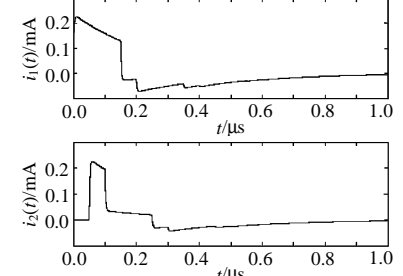
$$\mathbf{K}_{y2} = \begin{bmatrix} k_2 \left[(\cos f \sin q / c - CZ_0) \left(1 + \frac{R_1}{Z_0} \right) + \right. \\ \left. \frac{R_1}{Z_0} \cos f \sin q / c \right] \\ \left(1 - \frac{R_1}{Z_0} \right) (\cos f \sin q / c + CZ_0) \\ -k_1 \left(1 - \frac{R_1}{Z_0} \right) (\cos f \sin q / c + CZ_0) \end{bmatrix}; \\ \mathbf{S}_{y2} = \begin{bmatrix} h e_y[t - (T_2 + 2nT_0)] \\ h e_y[t - (T_1 + (2n+1)T_0)] \\ h e_y[t - (T_2 + (2n+2)T_0)] \end{bmatrix}.$$

2.2 仿真结果

应用式(10)(11)分析文献[16]中的例子, 假设均匀电磁波作用于传输线上, 电场强度为 $e(t) = 1.05 (e^{-4 \times 10^6 t} - e^{-4.76 \times 10^8 t}) \text{ V/m}$; $\alpha = 0^\circ$, 即该均匀平面波为垂直极化波。入射角为 60° , 方位角为 $\phi = 0^\circ$, 导体半径为 $a = 0.15 \text{ cm}$, 导体间距 $h = 0.2 \text{ m}$, 传输线长度 $l = 30 \text{ m}$ 。传输线特性阻抗为 $Z_0 = 293 \Omega$ 。本文称与来波对应的传输线一端为传输线的源端, 另一端称为负载端。本例中传输线源端和负载端的端接阻抗为 $Z_1 = Z_2 = 147 \Omega$ 。应用本文的推导公式(10)(11)进行仿真。结果如图 2 所示, 从波形对比可以看出本文的理论公式是正确的。



(a) 本文仿真结果



(b) 文献[16]仿真结果

图 2 传输线首末端耦合电流的仿真结果
Fig. 2 Simulation results of current at terminals of transmission line

仿真过程中发现式(10)(11)中 n 值不用取得过大, 解收敛的速度很快。本算例中 $n=6$, 因此对于大多数两导体组成的理想导体来说, 应用拉普拉斯变换方法计算简单, 速度快。为说明收敛速度, 本文给出了 $n=0$ 、 $n=1$ 和 $n=2$ 情况下的仿真结果, 如图 3 所示。图 3(a) 中 $n=0$ 时电流为 10^{-4} 数量级, 图 3(b) 中 $n=1$ 时电流为 10^{-5} 数量级, 图 3(c) 中 $n=2$ 时电流为 10^{-6} 数量级。因此可以看出该方法收敛很快。

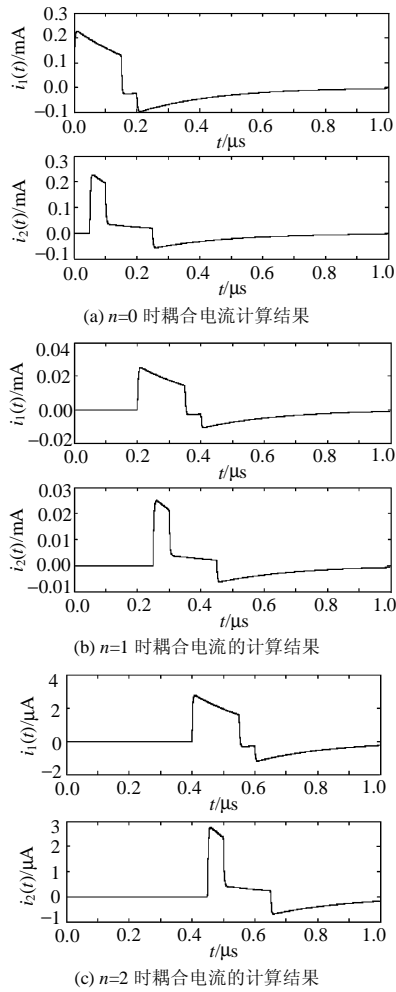


图 3 n 取不同值时耦合电流计算结果

Fig. 3 Simulation results of coupling current under different value of n

3 耦合电流大小与终端阻抗之间的关系

传输线参数以及入射场参数与第 2 节仿真例子相同。改变传输线两终端电阻, 分析终端电阻变化终端耦合电流大小的变化曲线。仿真中令两终端电阻分别以步长 $\Delta R=50\Omega$ 递增, 源端和负载端电阻分别取 100 个计算点。仿真波形如图 4 所示, 两水平坐标分别为源端电阻 Z_1 和负载端电阻 Z_2 对数形式,

电阻单位均为 Ω 。由于电阻变化范围很大, 水平两坐标用对数形式表示。上图纵坐标为源端电流最大值 $I_{1\max}$ 与入射电场强度最大值 E_0 比值, 下图纵坐标为负载端电流最大值 $I_{2\max}$ 与入射电场强度最大值比值, 单位为 $\text{mA}/(\text{V}/\text{m})$ 。可以看出, 源端和负载端电流随着对侧电阻的增加而增大, 且在总的变化趋势中基本上呈单调增加。

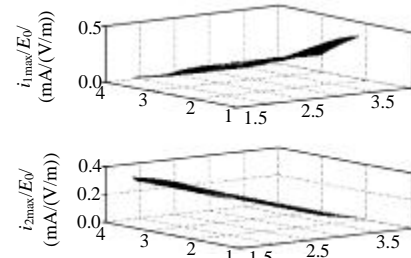


图 4 耦合电流最大值随终端电阻的变化曲线

Fig. 4 Variation curves of coupling currents with terminal resistance

4 结论

实际应用中存在很多以近似理想大地为回线的传输线。对于这类传输线应用拉氏域的方法可获得时域的半解析解。从仿真结果中可以看出, 耦合电流随着 n 值的增加按照 10 倍数量的关系衰减, 耦合电流收敛速度很快。应用该方法计算速度快、准确, 易于研究场线之间的耦合机理。传输线耦合电流随着传输线终端电阻的变化而变化, 在总的变化趋势中基本上呈单调增加。

参考文献

- [1] 卢斌先, 王泽忠, 李成榕, 等. 500 kV 变电站开关操作瞬态电场测量与研究[J]. 中国电机工程学报, 2004, 24(4): 133-138.
Lu Binxian, Wang Zezhong, Li Chengrong, et al. Measurement and research of switching operation transient electric field in 500 kV substations[J]. Proceedings of the CSEE, 2004, 24(4): 133-138(in Chinese).
- [2] 司大军, 杜洪春, 陈学允, 等. 输电线路雷击的电磁暂态特征分析及其识别方法研究[J]. 中国电机工程学报, 2005, 25(5): 64-69.
Si Dajun, Du Hongchun, Chen Xueyun, et al. Study on characteristics and identification of transients on transmission lines caused by lightning stroke[J]. Proceedings of the CSEE, 2005, 25(5): 64-69(in Chinese).
- [3] 吴桂芳. 我国±500 kV 直流输电工程的电磁环境问题[J]. 电网技术, 2005, 29(11): 5-8.
Wu Guifang. Electromagnetic environment problem brought about by ±500 kV substation DC transmission project in China[J]. Power System Technology, 2005, 29(11): 5-8(in Chinese).
- [4] Taylor C D, Satterwhite R S, Harrison C W. The response of a terminated two-wire transmission line excited by a nonuniform electromagnetic field[J]. IEEE Trans on Antennas Propagation, 1965,

- 3(6): 987-989.
- [5] Agrawal A K, Price H J, Gurbaxani S H. Transient response of multiconductor transmission lines excited by a nonuniform electromagnetic field[J]. IEEE Trans on Electromagnetic Compatibility, 1980, 22: 119-129.
- [6] Racchidi F. Formulation of field to coupling equations transmission line in terms of magnetic excitation field[J]. IEEE Trans on Electromagnetic Compatibility, 1994, 35(3): 404-407.
- [7] Tesche F M, Barnes P R. A multiconductor models for determining the response of power transmission line and distribution lines to a high altitude electromagnetic pulse (HEMP)[J]. IEEE Trans on Power Delivery, 1989, 4(3): 1955-1964.
- [8] Hansen D, Schaer H, Koenigstein D, et al. Response of an overhead wire near a NEMP simulator[J]. IEEE Trans on Electromagnetic Compatibility, 1990, 31(1): 18-27.
- [9] 谢彦召, 孙蓓云, 聂鑫, 等. 有界波电磁脉冲模拟器下短线缆效应的理论和实验研究[J]. 强激光与粒子束, 2005, 17(11): 1717-1720.
Xie Yanzhao, Sun Beiyun, Nie Xin, et al. Response of a short single-wire line illuminated by an EMP simulator[J]. High Power Laser and Particle Beams, 2005, 17(11): 1717-1720.
- [10] 谢彦召, 王赞基, 王群书. 地面附近架高线缆HEMP响应计算的Agrawal和Taylor模型比较[J]. 强激光与粒子束, 2005, 17(4): 575-580.
Xie Yanzhao, Wang Zanji, Wang Qunshu. Comparison of Agrawal and Taylor models for response calculations of above ground cable excited by HEMP[J]. High Power Laser and Particle Beams, 2005, 17(4): 575-580(in Chinese).
- [11] 莫付江, 陈允平, 阮江军. 架空输电线路雷击感应过电压耦合激励及计算方法分析[J]. 电网技术, 2005, 29(6): 72-77.

(上接第40页 continued from page 40)

- [10] 程其云, 孙才新, 周濂, 等. 粗糙集信息熵与自适应神经网络模糊系统相结合的电力负荷短期预测模型及方法[J]. 电网技术, 2004, 28(17): 73-75.
Cheng Qiyun, Sun Caixin, Zhou Quan, et al. Based on integration of information entropy in rough set theory with adaptive neural fuzzy inference system[J]. Power System Technology, 2004, 28(17): 73-75 (in Chinese).
- [11] 王志勇, 郭创新, 曹一家. 基于模糊粗糙集和神经网络的短期负荷预测方法[J]. 中国电机工程学报, 2005, 25(19): 7-11.
Wang ZhiYong, Guo ChuangXin, Cao Yijia. A method for short term load forecasting integrating fuzzy rough set with artificial neural network[J]. Proceedings of the CSEE, 2005, 25(19): 7-11(in Chinese).
- [12] 于达仁, 胡清华, 鲍文. 融合粗糙集和模糊聚类的连续数据知识发现[J]. 中国电机工程学报, 2004, 24(6): 205-210.
Yu Daren, Hu Qinghua, Bao Wen. Combining rough set methodology and fuzzy clustering for knowledge discovery from quantitative data [J]. Proceedings of the CSEE, 2004, 24(6): 205-210(in Chinese).
- [13] 张文修, 吴伟志. 粗糙集理论与方法[M]. 北京: 科学出版社, 2005.
- [14] 张文修, 仇国芳. 基于粗糙集的不确定决策[M]. 北京: 清华大学出版社, 2005.
- [15] 刘清. Rough集及 Rough 推理[M]. 北京: 科学出版社, 2005.
- [16] 程其云, 张晓星. 基于粗糙集数据挖掘的配电网小区空间负荷预测方法研究[J]. 电工技术学报, 2005, 20(5): 98-102.
- Mo Fujiang, Chen Yunping, Ruan Jangjun. Analysis on coupling mechanism and calculation method of lightning induced surge on overhead transmission lines[J]. Power System Technology, 2005, 29(6): 72-77(in Chinese).
- [12] D'Amore M, Sabrina M, Scarlatti A. Modeling of magnetic-field coupling with cable bundle harnesses[J]. IEEE Trans on Electromagnetic Compatibility, 2003, 45(3): 520-530.
- [13] Antonini G, Orlandi A. Spice equivalent circuit of a two-parallel-wires shielded cable for evaluation of the RF induced voltages at the terminations[J]. IEEE Trans on Electromagnetic Compatibility, 2004, 46(2): 189-198.
- [14] Tesche F M, Kalin A W, Brandli B, et al. Estimations of lightning-induced voltage stress within buried shielded conduits [J]. IEEE Trans on Electromagnetic Compatibility, 1998, 40(4): 492-503.
- [15] Kruse V J, Liu T K, Tesche F M. Flashover vulnerability of transmission and distribution lines to high altitude electromagnetic pulse(HEMP)[J]. IEEE Trans on Power Delivery, 1990, 5(2): 1164-1169.
- [16] Tesche F M, Ianoz M V, Karlsson T. EMC analysis methods and computational models[M]. New York: John Wiley & Sons, 2001.

收稿日期: 2007-05-16。

作者简介:

卢斌先(1969—), 男, 博士, 副教授, 从事电力系统电磁兼容、电磁测量等研究工作;

王泽忠(1960—), 男, 博士, 教授, 博士生导师, 主要从事电磁场数值计算、电力系统电磁兼容、电磁测量等研究工作;

程养春(1974—), 男, 博士, 副教授, 主要从事电力系统高压绝缘子在线检测等研究工作。

(责任编辑 马晓华)

Cheng Qiyun, Zhang Xiaoxing. Spatial load forecasting method for distribution net based on rough set data mining approach [J]. Transactions of China Electrotechnical Society, 2005, 20(5): 98-102(in Chinese).

[17] 吴蓓, 丁明. 基于模糊推理和多目标规划的空间负荷预测[J]. 电网技术, 2004, 28(15): 48-52.

Wu Bei, Ding Ming. Spatial load forecasting based on fuzzy reasoning and multi objective programming[J]. Power System Technology, 2004, 28(15): 48-52(in Chinese).

[18] Chow M Y, Tram H. Methodology of urban re-development considerations in spatial load forecasting[J]. IEEE Trans on Power Systems, 1997, 12(2): 996-1001.

[19] Chow M Y, Tram H. Application of fuzzy logic technology for spatial load forecasting[J]. IEEE Trans on Power Systems, 1997, 12(3): 1360-1366.

[20] Wu H C, Lu C N. A spatial modeling technique for small area load forecast[C]. Power Engineering Society Summer Meeting, 2001.

收稿日期: 2007-01-30。

作者简介:

熊 浩(1979—), 男, 博士研究生, 研究方向为人工智能领域在电力系统中的应用、高电压与绝缘监测、电磁兼容等, E-mail: thomasxiong@sina.com;

李卫国(1957—), 男, 教授, 博士生导师, 研究方向为人工智能、高电压与绝缘监测、电磁兼容等。

(编辑 杜宁)